

---

## SSLP320 - the purpose of Propagation of an emerging crack X-FEM solicited in Mode I

---

### Summarized

This test is validating the computation of the stress intensity factors ( $K_I$  and  $K_{II}$ ) and the way of crack propagation with X-FEM in 2D, in the frame of linear elasticity.

This test brings into play a rectangular plate with a crack leading, and subjected to a loading of tension to the edges inferior and superior of the plate.

Four methods to manage the propagation of cracks X-FEM are available. Each one of them is the object of a modelization.

Three modelizations are considered:

- modelization a: method MAILLAGE,
- modelization b: method SIMPLEXE,
- modelization C: method UPWIND,
- modelization D: method GEOMETRIQUE.

The relevance of the results is evaluated by comparison of the factors of intensity of the stresses with the analytical values.

One finds a variation enters  $K_I$  and  $K_{II}$  theoretical lower than 1,13% for all the methods.

## 1 Problem of reference

### 1.1 Geometry

the structure 2D is a rectangular 2D plate ( $LX=10\text{ m}$ ,  $LY=30\text{ m}$ ), comprising an emerging crack [Figure 1.1-a]. The length of initial crack is  $a=5\text{ m}$ .

One calls "line lower", line in  $y=0$  and "line higher", line in  $y=LY$ .

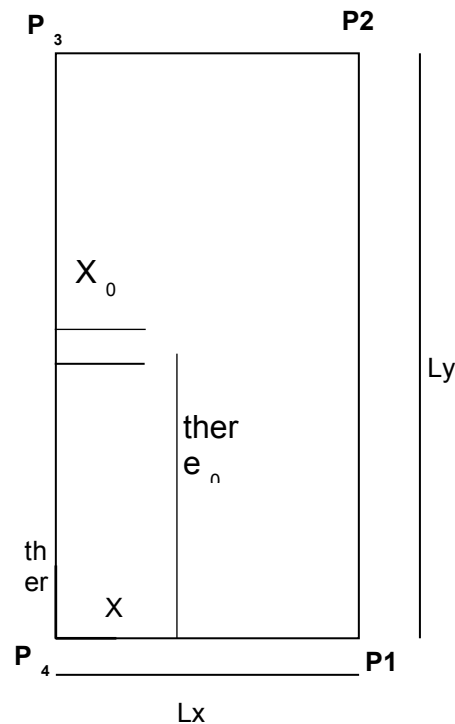


Figure 1.1-a : geometry of the fissured plate

the noted nodes  $P1$  and  $P4$  on Figure 1.1-a are used to impose the boundary conditions, which are clarified in the paragraph [§1.31.3].

### 1.2 Properties of the material

Modulus Young:  $E=205\ 10^9\ Pa$   
Poisson's ratio:  $\nu=0$

### 1.3 Boundary conditions and loadings

the loading consists in applying a distributed force to the lines lower and higher  $p=106\ Pa$  and in the meaning of the norm external to surface.

In order to block the rigid modes, one blocks displacements of the nodes  $P_1$ ,  $P_2$ ,  $P_3$  and  $P_4$  as follows:

- $DY^{P4} = DY^{P1} = 0$  ;
- $DX^{P4} = 0$

## 1.4 Reference solution

the analytical statements of the stress intensity factors  $K_I$  and  $K_{II}$  are functions of the distributed force  $p$ , length of crack  $a$ , width of the plate  $Lx$  [1]:

$$K_I = p \sqrt{\pi a} f\left(\frac{a}{Lx}\right)$$

$$K_{II} = 0$$

where the function  $f$  can be given several different ways. We choose that obtained by [1], and which is true for  $\frac{a}{Lx} < 0,6$  :

$$f\left(\frac{a}{Lx}\right) = 1,12 - 0,231\left(\frac{a}{Lx}\right) + 10,55\left(\frac{a}{Lx}\right)^2 - 21,72\left(\frac{a}{Lx}\right)^3 + 30,39\left(\frac{a}{Lx}\right)^4$$

One advances crack thanks to the model of Paris:

$\frac{da}{dN} = C \Delta K^m$  where  $a$  is the length of crack,  $C$  and  $m$  are constants of the material,  $\Delta K$  is the difference between two  $FICs$  consecutive and  $N$  is the number of cycles.

With the numerical values of the test:

No propagation: 0,25 m

$Lx$  : 10 m

Reference		
$a(m)$	$K_I (Pa.m^{0,5})$	$K_{II} (Pa.m^{0,5})$
2,5	4,205998 106	0
2,75	4,63286 106	0
3	5,09492 106	0
3,25	5,59908 106	0,3,5
	6,15349 106	0
3,75	6,76776 106	0
4	7,4531 106	0
4,25	8,2224 106	0,4,5
	9,0905 106	0
4,75	1,0074 107	0
5	1,1192 107	0
5,25	1,2465 107	0,5,5
	1,3916 107	0
5,75	1,55716 107	0
6	1,74586 107	0

Table 1.4-1 : values of reference de for  $K_I$  and  $K_{II}$

## 1.5 Bibliography

- 1.TADA H., PARIS P., IRWIN G.: The stress analysis of aces, Handbook. Del Research Corporation, Hellertown, Pennsylvania, 1973

## 2 Modelization a: Method mesh

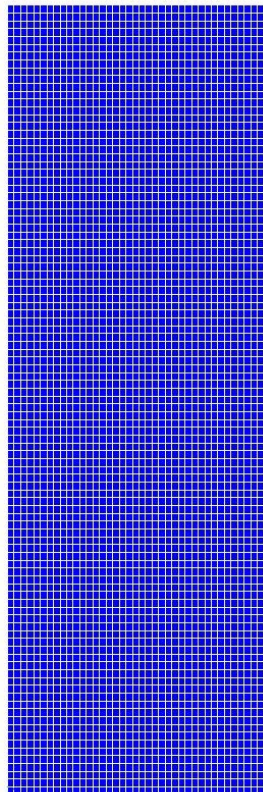
---

### 2.1 Characteristics of the modelization

In this modelization, the method `MAILLAGE` is tested for the crack propagation. The level-sets are determined by orthogonal projection on the segments composing crack.

### 2.2 Characteristics of the mesh

the structure is modelled by a "healthy" mesh regular composed of  $40 \times 101$  `QUAD4`, respectively along the axes  $x, y$ . The crack is represented by a succession of `SEG2`, independently of the mesh of structure.



Appear 2.2-a : mesh of the fissured plate

### 2.3 Quantities tested and results

For each step of propagation ( $2,5 m$ ), one tests the value of the stress intensity factors  $K_I$  and  $K_{II}$  data by `CALC_G`.

One also tests the Y-coordinate of the crack tip given by `PROPA_FISS`.

## 2.3.1 Results on $K_I$ :

Identification	Code_Aster	Reference	difference
CALC_G			
KI_1	4,17448 106	4,205998 106	-0,749%
KI_2	4,60197 106	4,63286 106	-0,667%
KI_3	5,0668 106	5,09492 106	-0,552%
KI_4	5,575 106	5,59908 106	-0,43%
KI_5	6,1334 106	6,15349 106	-0,326%
KI_6	6,7499 106	6,76776 106	-0,264%
KI_7	7,4338 106	7,4531 106	-0,259%
KI_8	8,19599 106	8,2224 106	-0,322%
KI_9	9,0497 106	9,0905 106	-0,449%
KI_10	1,0011 107	1,0074 107	-0,627%
KI_11	1,1099 107	1,1192 107	-0,828%
KI_12	1,2339 107	1,2465 107	-1,011%
KI_13	1,37603 107	1,3916 107	-1,121%
KI_14	1,54018 107	1,55716 107	-1,09%
KI_15	1,7313 107	1,74586 107	-0,834%

## 2.3.2 Results on $K_{II}$ :

For this test, it is wished that  $K_{II}$  be lower than  $10^{-4} K_I$ . Thus, one makes sure that  $K_{II}$  is rather close to zero, the value of reference.

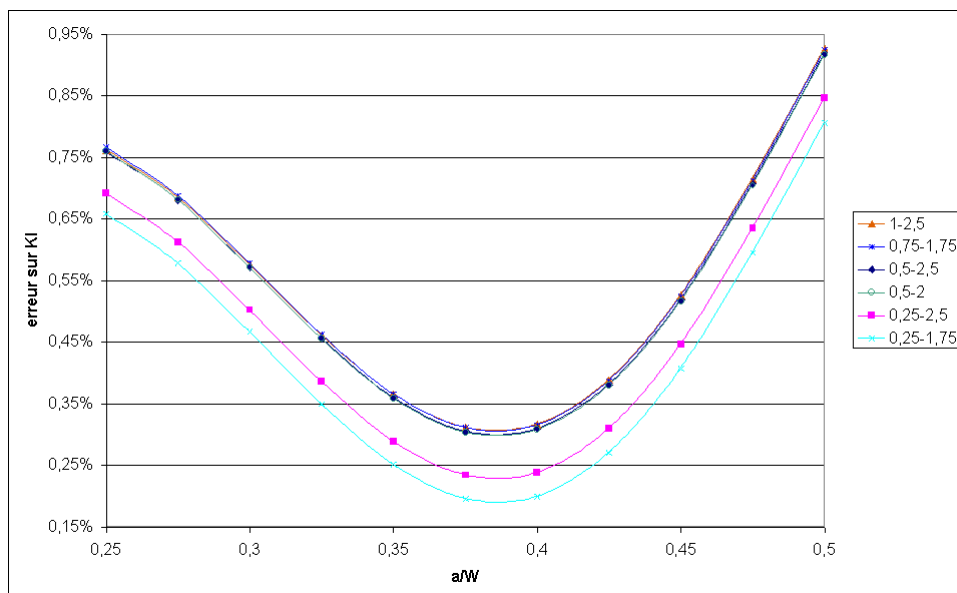
Identification	Code_Aster	Reference
CALC_G		
KII_1	-2,7313 102	0
KII_2	-8,5062 101	0
KII_3	-2,6061 102	0
KII_4	1,5995 102	0
KII_5	-2,7309 102	0
KII_6	-2,3176 102	0
KII_7	-3,1276 102	0
KII_8	3,1327 102	0
KII_9	-3,8393 102	0
KII_10	-4,1916 102	0
KII_11	-4,986 102	0
KII_12	-5,6998 102	0
KII_13	-6,7642 102	0
KII_14	-7,9542 102	0
KII_15	-9,5344 102	0

## 2.3.3 Results on the Y-coordinate of the crack tip:

It is checked that the coordinates in Y-coordinate of the successive crack tips are close to the initial value. This checking gives the same indications as the test on  $K_{II}$ .

Identification	Code_Aster	Reference	complementary
Difference			
CALC_G	y_1	15	
15.0%	y_2	15	15 2,18 <sup>10</sup>
4%	y_3	15	15.2,8 <sup>10</sup>
4%	y_4	15	15 4,51 <sup>10</sup>
4%	y_5	15	15 5,47 <sup>10</sup>
4%	y_6	15	15 6,95 <sup>10</sup>
4%	y_7	15	15.8,1 <sup>10</sup>
4%	y_8	15	15.9,5 <sup>10</sup>
4%	y_9	15,0002	15
0,001%	y_10	15,0002	15
0,001%	y_11	15,0002	15
0,001%	y_12	15,0002	15
0,002%	y_13	15,0002	15
0,002%	y_14	15,0003	15
0,002%	y_15	15,0003	15

## 2.4 0,002% Results



Appears 2.4-a : Influence choice of contours IH and RS on the error on KI

We can see here that the configuration most adapted for the choice of  $RI$  and  $RS$  (contours lower and higher of the field theta) is:  $RI=2*L_0$  and  $RS=7*L_0$  where  $L_0$  is the smallest edge of the mesh.

## 3 Modelization b: Method simplex

### 3.1 Characteristics of the modelization

In this modelization, method `SIMPLEXE` is tested for the crack propagation.  
The level-sets are determined by resolution of the equations of reactualization.

### 3.2 Characteristics of the mesh

One uses here the same mesh as in the modelization A (§2.1).

### 3.3 Quantities tested and results

For each step of propagation, one tests the value of the stress intensity factors  $K_I$  and  $K_{II}$  data by `CALC_G`.

#### 3.3.1 Results on $K_I$ :

Identification	Code_Aster	Reference	difference
CALC_G			
KI_1	4,17448	4,205998 106	-0,749%
KI_2	4,60197	4,63286 106	-0,667%
KI_3	5,06681	5,09492 106	-0,552%
KI_4	5,57501	5,59908 106	-0,43%
KI_5	6,13343	6,15349 106	-0,326%
KI_6	6,74995	6,76776 106	-0,263%
KI_7	7,43384	7,4531 106	-0,258%
KI_8	8,19608	8,2224 106	-0,32%
KI_9	9,04986	9,0905 106	-0,447%
KI_10	1,00111	1,0074 107	-0,625%
KI_11	1,10996	1,1192 107	-0,825%
KI_12	1,23393	1,2465 107	-1,008%
KI_13	1,37608	1,3916 107	-1,117%
KI_14	1,54026	1,55716 107	-1,085%
KI_15	1,73142	1,74586 107	-0,827%

## 3.3.2 Results on $K_{II}$ :

Identification	Code_Aster	Reference
CALC_G		
KII_1	-2,7313 102	0
KII_2	-2,9582 102	0
KII_3	-3,3848 102	0
KII_4	-3,9204 102	0
KII_5	-4,4895 102	0
KII_6	-5,0302 102	0
KII_7	-5,4802 102	0
KII_8	-5,7767 102	0
KII_9	-5,8608 102	0
KII_10	-5,7002 102	0
KII_11	-5,2708 102	0
KII_12	-4,5292 102	0
KII_13	-3,422 102	0
KII_14	-1,8819 102	0
KII_15	-1,7862 101	0



## 4 Modelization C: Method upwind

### 4.1 Characteristic of the modelization

In this modelization, method UPWIND is tested for the crack propagation.

The level-sets are determined by resolution of the equations of reactualization per diagram to the finite differences.

### 4.2 Characteristics of the mesh

One uses here the same mesh as in the modelization A (§2.1).

### 4.3 Quantities tested and results

For each step of propagation, one tests the value of the stress intensity factors  $K_I$  and  $K_{II}$  data by CALC\_G.

#### 4.3.1 Results on KI:

Identification	Code_Aster	Reference	difference
CALC_G			
KI_1	4.17448E+06	4,205998 106	-0,749%
KI_2	4.60197E+06	4,63286 106	-0,667%
KI_3	5.06680E+06	5,09492 106	-0,552%
KI_4	5.57500E+06	5,59908 106	-0,43%
KI_5	6.13340E+06	6,15349 106	-0,326%
KI_6	6.74991E+06	6,76776 106	-0,264%
KI_7	7.43378E+06	7,4531 106	-0,259%
KI_8	8.19599E+06	8,2224 106	-0,322%
KI_9	9.04972E+06	9,0905 106	-0,449%
KI_10	1.00110E+07	1,0074 107	-0,627%
KI_11	1.10993E+07	1,1192 107	-0,828%
KI_12	1.23389E+07	1,2465 107	-1,011%
KI_13	1.37603E+07	1,3916 107	-1,122%
KI_14	1.54018E+07	1,55716 107	-1,09%
KI_15	1.73130E+07	1,74586 107	-0,834%

## 4.3.2 Results on KII:

Identification	Code_Aster	Reference
CALC_G		
KII_1	-2,7313 102	0
KII_2	-2,8454 102	0
KII_3	-3,0026 102	0
KII_4	-3,2069 102	0
KII_5	-3,4643 102	0
KII_6	-3,7828 102	0
KII_7	-4,1724 102	0
KII_8	-4,6462 102	0
KII_9	-5,2209 102	0
KII_10	-5,9177 102	0
KII_11	-6,7643 102	0
KII_12	-7,7966 102	0
KII_13	-9,0621 102	0
KII_14	-1,0624 103	0
KII_15	-1,2568 103	0

## 5 Modelization D: Geometrical method

### 5.1 Characteristics of the modelization

In this modelization, method GEOMETRIQUE is tested for the crack propagation.  
The level-sets are recomputed with each step of propagation.

### 5.2 Characteristics of the mesh

One uses here the same mesh as in the modelization A (§2.1).

### 5.3 Quantities tested and results

For each step of propagation, one tests the value of the stress intensity factors  $K_I$  and  $K_{II}$  data by CALC\_G.

#### 5.3.1 Results on KI:

Identification	Code_Aster	Reference	Difference
CALC_G			
KI_1	4,174476 106	4,205998 106	-0,749%
KI_2	4,601963 106	4,63286 106	-0,667%
KI_3	5,066799 106	5,09492 106	-0,522%
KI_4	5,574998 106	5,59908 106	-0,430%
KI_5	6,133404 106	6,15349 106	-0,326%
KI_6	6,749911 106	6,76776 106	-0,264%
KI_7	7,433777 106	7,4531 106	-0,259%
KI_8	8,195987 106	8,2224 106	-0,322%
KI_9	9,049722 106	9,0905 106	-0,449%
KI_10	1,001096 107	1,0074 107	-0,627%
KI_11	1,109928 107	1,1192 107	-0,828%
KI_12	1,233893 107	1,2465 107	-1,01%
KI_13	1,376027 107	1,3916 107	-1,12%
KI_14	1,540181 107	1,55716 107	-1,09%
KI_15	1,731302 107	1,74586 107	-0,834%

## 5.3.2 Results on KII:

Identification	Code_Aster	Reference
CALC_G		
KII_1	0,0	0
KII_2	1,30 X 10 <sup>2</sup>	0
KII_3	0,0	0
KII_4	2,48 X 10 <sup>1</sup>	0
KII_5	0,0	0
KII_6	0,0	0
KII_7	0,0	0
KII_8	0,0	0
KII_9	0,0	0
KII_10	0,0	0
KII_11	0,0	0
KII_12	0,0	0
KII_13	0,0	0
KII_14	0,0	0
KII_15	0,0	0

## 6 Summaries of the Performance

---

### 6.1 results of the methods

One can compare the computing time for the same number of steps of propagation (15) of the four methods. It is noticed here that method `GEOMETRIQUE` is definitely faster than the three other methods for the same discretization.

Mesh	Method	Time ( s )
40×101	MAILLAGE	129
	SIMPLEXE	290
	UPWIND	244
	GEOMETRIQUE	30

### 6.2 Conclusion

the purposes of this test are reached:

- `MAILLAGE` to validate on a simple case the computation of the stress intensity factors in *I* mode for elements X-FEM for the four methods, `SIMPLEXE`, `UPWIND` and `GEOMETRIQUE`.
- to distinguish the best method for this case. For equal results, the geometrical method is most powerful. One thus recommends here to choose this method for this case.